

Inhibition of N-myc downstream-regulated gene 2 in prostatic carcinoma

Chuigong Yu,^{1,2,†} Guojun Wu,^{2,†} Nana Dang,^{1,†} Wei Zhang,¹ Rui Zhang,¹ Wei Yan,³ Yi Zhao,² Lei Gao,² Yingmei Wang,³ Noor Beckwith,⁴ Jianlin Yuan^{2,*} and Libo Yao^{1,*}

¹Department of Biochemistry and Molecular Biology; State Key Laboratory of Cancer Biology; ²Department of Urology; ³Department of Pathology; State Key Laboratory of GI Cancer Biology; Xijing Hospital; Fourth Military Medical University; Xi'an, China; ⁴Organismic & Evolutionary Biology; Harvard University; Cambridge, MA USA

[†]These authors contributed equally to this work.

Key words: NDRG2, c-Myc, inhibition, prostatic carcinoma, adenovirus, carcinogenesis, gene therapy

Abbreviations: GAPDH, glyceraldehyde phosphate dehydrogenase; MTT, methyl thiazolyl tetrazolium; DMSO, dimethyl sulphoxide; FCM, flow cytometry assays; TEM, transmission electron microscopy; TUNEL, TdT-mediated dUTP nick end labeling

To study the expression of N-myc Downstream Regulated Gene-2 (NDRG2) in prostatic carcinoma (PCA) tissue and in different PCA cell lines, and to investigate its clinical and pathological implications, 144 PCA and benign prostatic hyperplasia (BPH) tissue sections were analyzed retrospectively with immunohistochemistry (S-P method). The expression levels of NDRG2 and c-Myc in prostate cell lines were detected through protein gel blot. The effects of adenovirus-mediated NDRG2 on PC3 cells and PC3 nude mouse xenografts was observed through cell growth curves, tumor growth curves, flow cytometry (FCM), transmission electron microscopy (TEM) and TUNEL staining. The NDRG2 gene was highly expressed in BPH tissues, but not in carcinomatous ones ($\chi^2 = 25.98$, $p < 0.001$). Furthermore, positive expression of NDRG2 was negatively correlated with the Gleason score ($r = -0.445$, $p < 0.001$) and the c-myc level ($r = -0.311$, $p < 0.001$). However, positive expression of NDRG2 was not correlated with pTNM tumor stages or the serum concentration of prostate-specific antigen (PSA) ($p > 0.05$). The expression of the NDRG2 genes was low in the three PCA cell lines. PC3 cells infected by pAD-cmv-NDRG2 showed inhibition of proliferation both in vitro and in vivo. To sum up, NDRG2 may be involved in the carcinogenesis and progression of PCA. Moreover, adenovirus-mediated NDRG2 can suppress the proliferation of PC3 cells significantly both in vitro and in vivo. These results indicate that NDRG2 may become a new target gene for PCA diagnosis and therapy.

Introduction

Prostate carcinoma (PCA) is one of the most common malignant tumors in Europe and the United States. If it could be diagnosed earlier and treated surgically in time, fewer patients would have their lives cut short by inoperable tumors and poor prognoses. However, many tumors are diagnosed in advanced stages by which point they have become inoperable. Endocrine therapy is an alternative method to surgery in such cases, but the efficacy of the therapy has often been unsatisfying due to resistance. Therefore, it is vital to identify more genes that are specifically linked to PCA, so that we may expand our understanding of this disease and assist in the development of new diagnostic indicators and new targets for therapy.¹

NDRG was initially discovered overexpressing in N-myc knockout mice. Accordingly, it was named the 'N-myc downstream-regulated gene'.² The family of human *NDRGs* consists of four members: *NDRG1*, *NDRG2*, *NDRG3* and *NDRG4*. The

amino acid sequence homology within the human *NDRG* family is 57–65%, indicating that function is conserved.³ The human *NDRG2* gene (AF 159092) was first identified in our university's biochemistry laboratory and it was demonstrated to be a candidate tumor suppressor gene.⁴ *NDRG2* is located at 14q11.2 and contains 16 exons and 15 introns. *NDRG2* mRNA is composed of 2,024 bp and encodes a protein of 357 amino acids (41 kDa) with unconfirmed functions.⁵ However, some previous research has indicated that the expression of *NDRG2* decreased in various carcinomas including colon cancer, thyroid cancer, glioblastoma and renal cell carcinoma.^{6–10} The decrease suggests that *NDRG2* might play an important role in the morbidity of carcinomas. Furthermore, *NDRG2* has been verified to be involved in cell growth and differentiation; it may regulate myoblast proliferation and induce the differentiation of dendritic cells.^{11,12}

As *NDRG2* might play a crucial role in carcinogenesis and no research has been made into connections between *NDRG2* and PCA, we decided to investigate the expression of NDRG2 to

*Correspondence to: Libo Yao and Jianlin Yuan; Email: bioliboyao@163.com and jianliny@fmmu.edu.cn
Submitted: 03/29/11; Revised: 05/04/11; Accepted: 05/06/11
DOI: 10.4161/cbt.12.4.16382

Table 1. Expression of NDRG2 in BPH and PCA tissues

Group	NDRG2(-)	NDRG2(+)	χ^2 value	p value
BPH	7	30	25.98	< 0.001
PCA	72	35		

Data are presented as n (number of samples). Statistical significance was evaluated with χ^2 test.

Table 2. Relationship between expression of NDRG2 and PCA characteristics

Characteristic	Expression level of NDRG2				r value	p value
	-	+	++	+++		
Gleason score						
2 ~ 4	2	5	2	2		
5 ~ 7	39	12	10	-	-0.445	< 0.001
8 ~ 10	31	4	-	-		
pTNM stage						
pT1 ~ pT2	44	9	10	2		
pT3 ~ pT4	28	12	2	-	-0.038	0.303
PSA in serum						
≤20 ng/ml	14	11	1	1	-0.088	0.367
>20 ng/ml	58	10	11	1		

Data are presented as n (number of samples). Statistical significance was evaluated with Pearson correlation coefficient test.

determine its role in PCA. Using immunochemistry, we analyzed benign prostatic hyperplasia (BPH) and PCA, finding that PCA tissues have lower expression levels and lower positive expression percentage than BPH tissues. Next, we confirmed that PCA cell lines had lower protein expression levels of NDRG2 by protein gel blot. Finally, we used growth tests to show that NDRG2 could inhibit PCA in vitro and in vivo.

Results

Differential expression of NDRG2 in BPH and PCA tissues.

As is shown in Table 1, the rate of NDRG2 positive expression in BPH specimens was 81.08% (30/37), which was significantly higher than that in PCA tissues 32.71% (35/107) ($\chi^2 = 25.98$, $p < 0.001$). Moreover, expression of NDRG2 and Gleason scores were negatively correlated ($r = -0.445$, $p < 0.001$) (Table 2). That is to say, an increase in Gleason score generally meant a decrease in the percentages and levels of NDRG2 positive expression. Immunohistochemistry showed NDRG2 protein in the cytoplasm of BPH and PCA epithelia (Fig. 1A). The c-Myc protein was expressed in the cytoplasm of early-stage carcinomatous epithelia, but was more easily detected in nuclei upon the development of PCA. NDRG2 positive expression was not correlated with pathological Tumor-Node-Metastasis (pTNM) stage or serum PSA concentration ($p > 0.05$) (Table 2). The expression levels of NDRG2 were, however, negatively correlated with those of c-Myc ($r = -0.311$, $p < 0.001$) (Figs. 1B and 2).

Differential expression of NDRG2 in normal and carcinomatous prostate cell lines. The protein gel blot results showed

that all the three PCA cell lines expressed lower levels of NDRG2 protein than the normal human prostate cells (RWPE2), and that PC3 had the lowest level among the three PCA cell lines (Fig. 3A and B). The pattern of c-Myc protein expression was the opposite of that of NDRG2; the expression of c-Myc protein could hardly be detected in RWPE2, but easily detected in the three PCA cell lines, and PC3 possessed the highest level (Fig. 3A and B).

Adenovirus infection and cell growth inhibition tests.

Protein gel blot showed that PC3 cells were successfully targeted for infection. The most suitable infection conditions were concluded to be 20 MOI, and fluorescence microscopy was used 48 h after infection. Protein gel blots indicated that the pAd-cmv-NDRG2 adenovirus could cause overexpression NDRG2 protein in PC3 cells (Fig. 4A and B). The cell growth curves showed that NDRG2 could suppress the growth of PC3 cells more than that of the other two groups. The inhibition occurred at 36 h and became more and more powerful from then ($F \geq 12.43$, $p \leq 0.01$) (Fig. 5). The FCM results showed that PC3 cells infected with pAd-cmv-NDRG2 adenovirus were more easily arrested in G_0/G_1 cycle than the negative control and pAd-cmv-lacZ groups (48 h: $F = 56.64$, $p < 0.001$; 72 h: $F = 41.29$, $p < 0.001$) (Fig. 6A and Table 3). The protein gel blot results showed that NDRG2 could downregulate cyclinD1 and CDK4, and upregulate p21 in PC3 cells (Fig. 4A and B). The percentage of apoptotic cells in the NDRG2 group was larger than in the other two groups (48 h: $F = 22.28$, $p < 0.001$; 72 h: $F = 41.19$, $p < 0.001$) (Fig. 6B and Table 3). The TEM micrographs showed that the nuclei became smaller and heterochromatin increased in the NDRG2 group compared with the lacZ controls. Karyoplasm was concentrated and karyotheca was crumpled. The chromosome condensed into a semilunar shape and was clinging to the karyotheca and cellular membrane. All these apoptotic phenomena could be detected at both 48 and 72 h, though they were more typical at 72 h (Fig. 7).

Growth inhibition assays in vivo. Tumors were allowed to grow for 20 d after inoculation with PC3 cells (median size = 200 mm³ in each group). Six mice in each group survived after the injections with adenovirus. Tumor growth curves showed that NDRG2 could suppress the growth of PC3 inoculated tumors (Fig. 8A). The discrepancy had statistical significance from 6 d onwards ($F \geq 6.61$, $p < 0.01$) (Fig. 8B). The weight of tumors receiving pAd-cmv-NDRG2 was significantly lighter than that of pAd-cmv-lacZ or PBS-treated tumors ($F \geq 32.21$, $p < 0.001$) (Fig. 8C). The tumor mass to mouse mass ratio indicated that the physical condition of the mice in NDRG2 group was much better than that of the mice in the other groups ($F = 21.99$, $p < 0.001$) (Fig. 8D). Protein gel blot showed that pAd-cmv-NDRG2 adenovirus could upregulate expression of NDRG2 protein in the tumors (Fig. 9A and B). TUNEL stain results demonstrated that more apoptotic cancer cells were positive for TUNEL labeling in tumor tissues of the NDRG2-treated group, compared with the control groups ($F = 26.08$, $p < 0.001$) (Fig. 9C and D). The TEM micrographs indicated that the changes in the PC3 cells in the inoculated tumors treated with pAd-cmv-NDRG2 were similar to those seen in vitro (Fig. 9E).

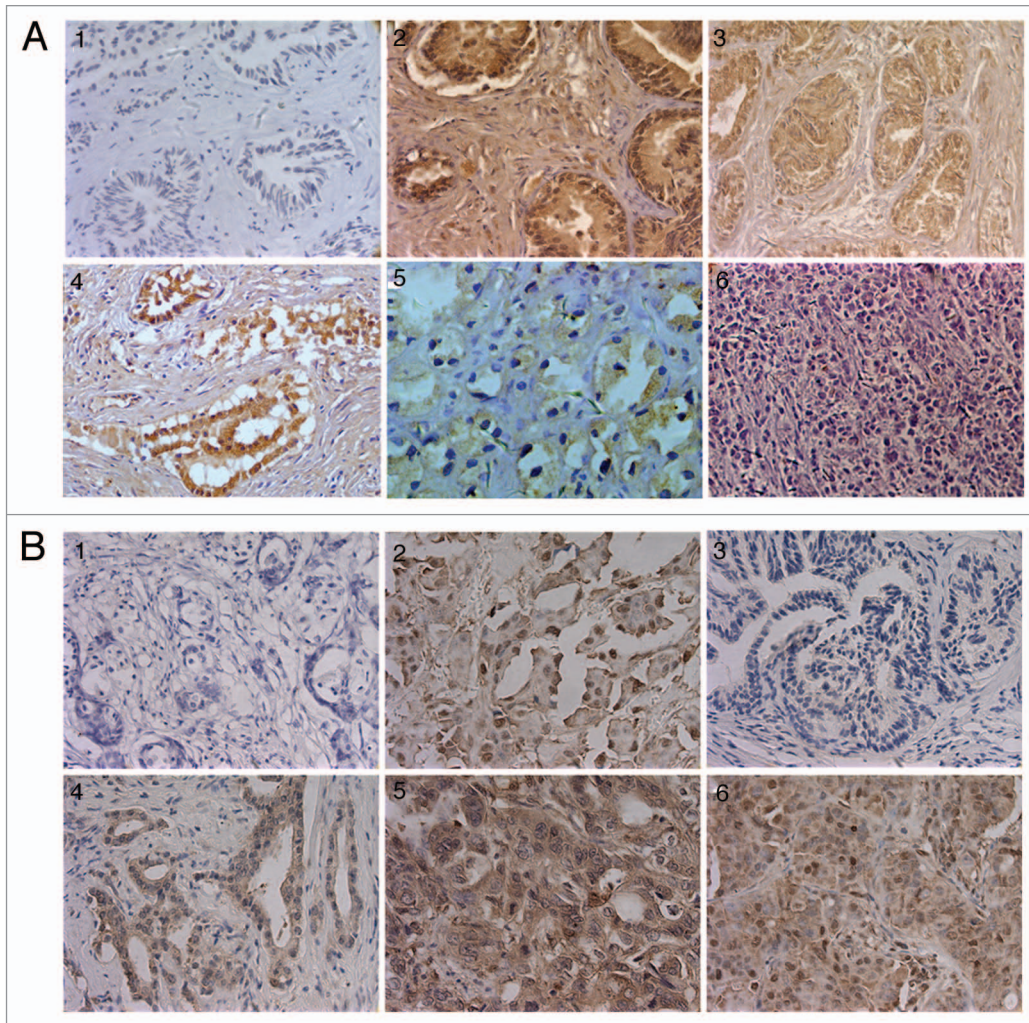


Figure 1. The expression of NDRG2 and c-Myc protein in prostate tumor tissues detected with immunohistochemistry staining. (A) The expression levels of NDRG2 protein decreases with increasing Gleason scores (x400). (1) Negative control; (2) positive control; (3) BPH tissue; (4–6) PCA tissues (Gleason score: 2 + 2 = 4, 3 + 4 = 7, 4 + 5 = 9, respectively). (B) The expression levels of c-Myc increases with increasing of Gleason scores (x400). (1) Negative control; (2) Positive control (breast cancer tissue); (3) BPH tissues; (4–6) PCA tissues (Gleason score: 2 + 2 = 4, 3 + 4 = 7, 4 + 5 = 9, respectively). The sections of (B) (3–6) originated from the same paraffin blocks as (A) (3–6) respectively, but visual fields were chosen to allow easier interpretation.

Discussion

Managing advanced PCA is challenging, and the median survival in hormone-resistant PCa (HRPC) is still less than 2 years.¹³ Approved systemic chemotherapies for HRPC provide limited benefits.¹⁴ Therefore, facilitating early diagnosis and finding new therapies are crucial goals in the study of PCA. *NDRG2* might be such a gene, one that should not be neglected, for a series of studies have implied that *NDRG2* plays an important role in cell proliferation and differentiation.^{15,16} Some significant phenomena found in our studies might partially prove this. Our previous studies have shown that the expression of *NDRG2* has negative correlation with c-Myc, the well known oncogene in neuroglioma cells, and c-Myc may repress *NDRG2* via Miz-1-dependent interaction.^{3,17} C-Myc was also verified to be a crucial oncogene in prostatic carcinoma development.¹⁸

Our data in this experiment indicate that *NDRG2* plays a role in PCA similar to its role in other malignant tumors. Immunohistochemistry results showed that the positive expression percentage of *NDRG2* in PCA tissues was significantly lower than that in BPH tissues. The expression levels of *NDRG2* protein decreased as the degree of PCA malignancy increased. We also found that the expression of *NDRG2* was negatively correlated with c-Myc in prostate tumors, just as it is in neuroglioma cells. Furthermore, the *NDRG2* expression levels in PCA cell lines (PC3, LNCaP and DU145) were lower than those in the normal prostate cell line (RWPE2). Adenovirus-mediated *NDRG2* was able to inhibit the PC3 cells' proliferation and promote their apoptosis both in vitro and in vivo. Overexpression of *NDRG2* affected the expression of several proteins (cyclin-D1, CDK4 and p21) that are important in cell cycle regulation and apoptosis, and overall *NDRG2* improved

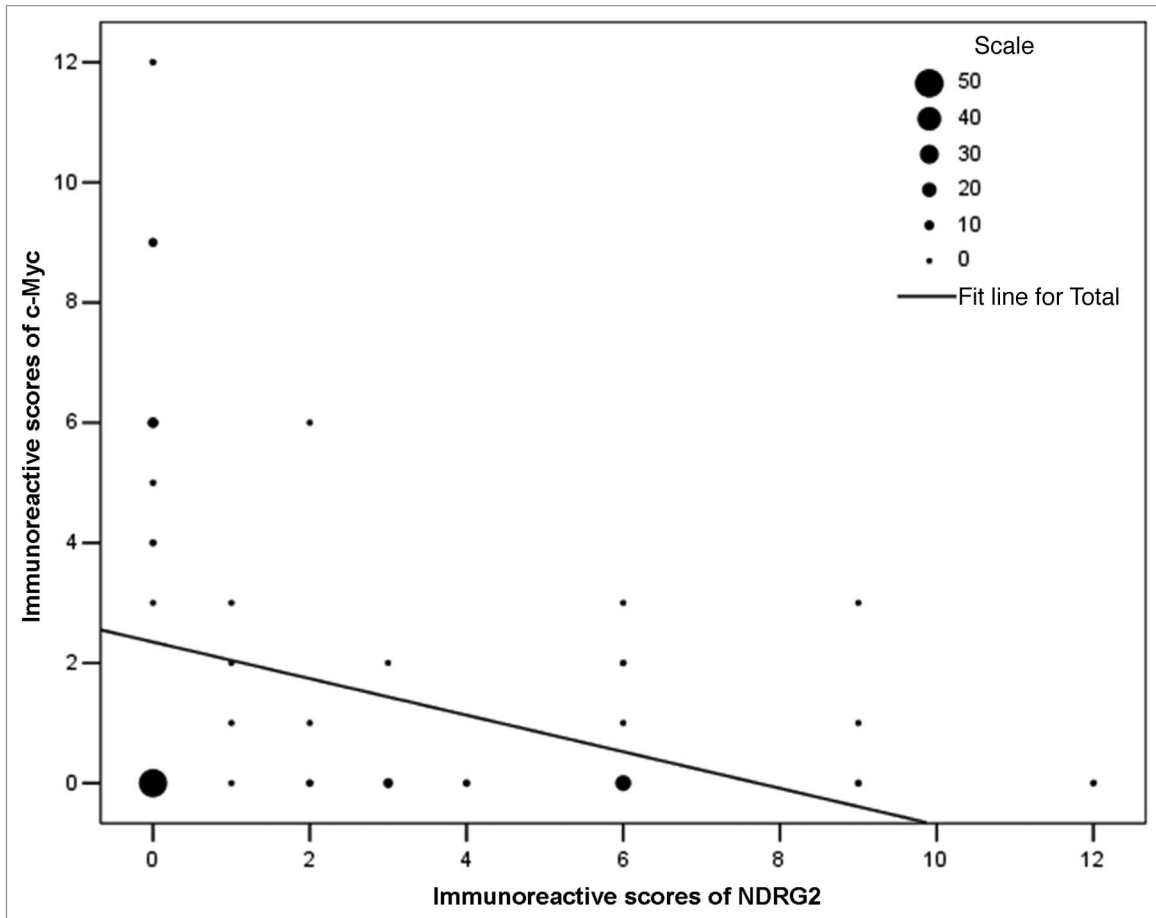


Figure 2. The expression levels of NDRG2 are negatively correlated with those of c-Myc. The number of specimen was shown as 'scale'. Disparities across groups were analyzed using Pearson correlation coefficient and the graph was generated by SPSS13.0 software. ($r = -0.311$, $p < 0.001$).

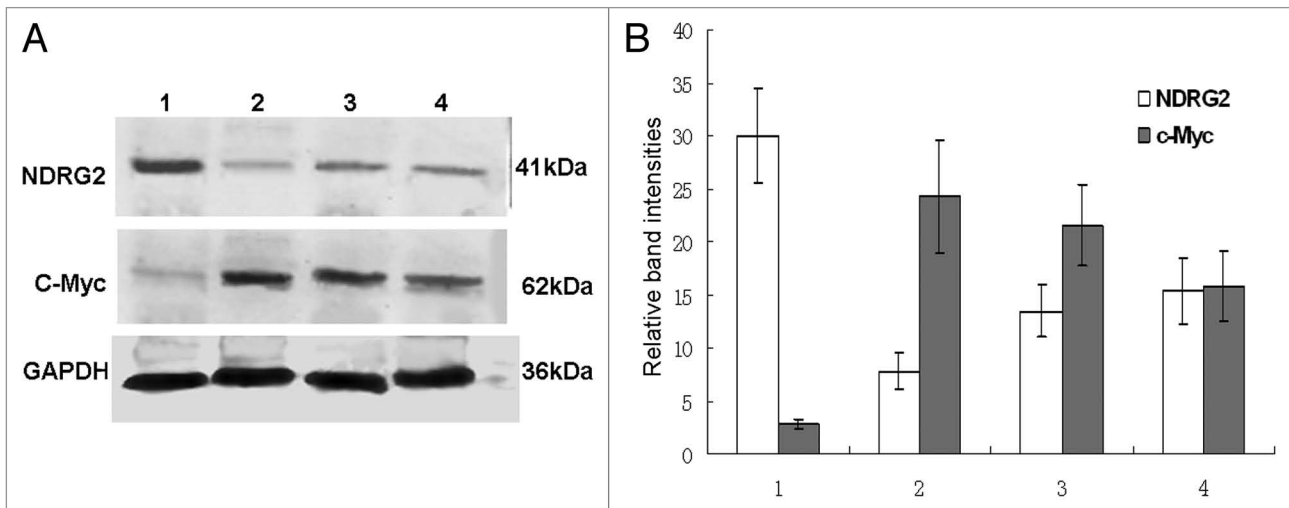


Figure 3. Differential expression of NDRG2 among prostate cell lines. (A) Expression level of NDRG2 and c-Myc protein as assayed by protein gel blot. (B) Relative quantification of NDRG2 and c-Myc protein expression, normalized to GAPDH levels. Lane 1: RWPE2; lane 2: PC3; lane 3: LNCaP; lane 4: DU145. GAPDH, glyceraldehyde-3-phosphate dehydrogenase. The results of protein gel blot were analyzed with Kodak Digital Science one-dimensional software. The figure shows the tendency of each group as indicated. All of the assays were repeated in at least three independent experiments. The results are shown as the mean \pm SD.

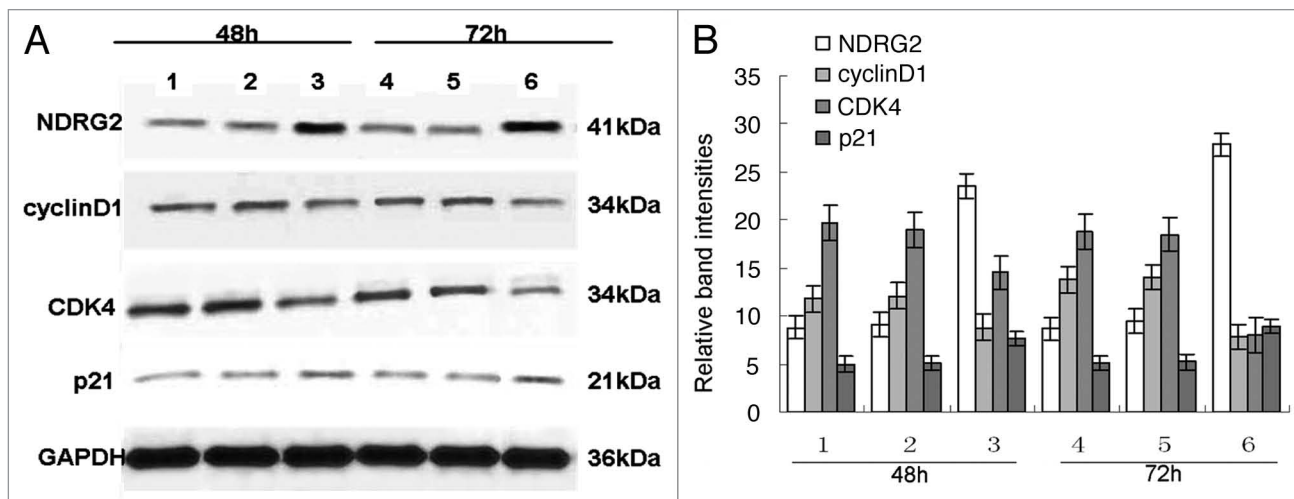


Figure 4. The influences of NDRG2 overexpression induced by adenovirus on PC3 cells. (A) The effect of NDRG2 overexpression on G₁ cell cycle and apoptosis regulators as assayed by protein gel blot. (B) Relative quantification of NDRG2 and other regulatory protein expression, normalized to GAPDH levels. (1–3) 48 h after the infection; (4–6) 72 h after the infection; (1 and 4) blank control (PBS); (2 and 5) LacZ; (3 and 6) NDRG2. Protein gel blots were analyzed with Kodak Digital Science one-dimensional software. The figure shows the tendency of each group as indicated. All the assays were repeated in at least three independent experiments. The results are shown as the mean \pm SD.

the physical condition of mice with inoculated tumors.

All of this implies that *NDRG2* may be involved in tumor morbidity and progression in many cancers, including PCA. *NDRG2* may perform its function through regulating the cell cycle and/or cell apoptosis. *NDRG2* has also been demonstrated in our experiments on prostate tumors to be negatively correlated with the well known oncogene *c-Myc*. The thesis that human *NDRG2* acts as a candidate tumor suppressor gene is thus feasible.⁴ However, whether the downregulation of *NDRG2* in PCA is a cause or a consequence remains presently unclear. Further studies are needed to investigate how *NDRG2* is involved in the progression from normal prostate tissue to PCA tissue. With continued research into *NDRG2*, the gene might prove to be a powerful tool in PCA diagnosis and therapy in the future.

Materials and Methods

Clinical collection of prostatic samples. A total of 144 PCA and BPH samples were collected, comprised of 37 BPH and 107 PCA samples. Human prostatic tumor tissues were collected between 2006 and 2008 from patients with prostatic tumors. All the patients were yellow race male from China. The range of donor age was 50–89 years, with a mean of 65.7 ± 8.9 years. Before treatments, the tissues were gathered by transurethral resection or needle biopsy in the Department of Urologic Surgery, Xijing Hospital, FMMU (Xi'an, China).

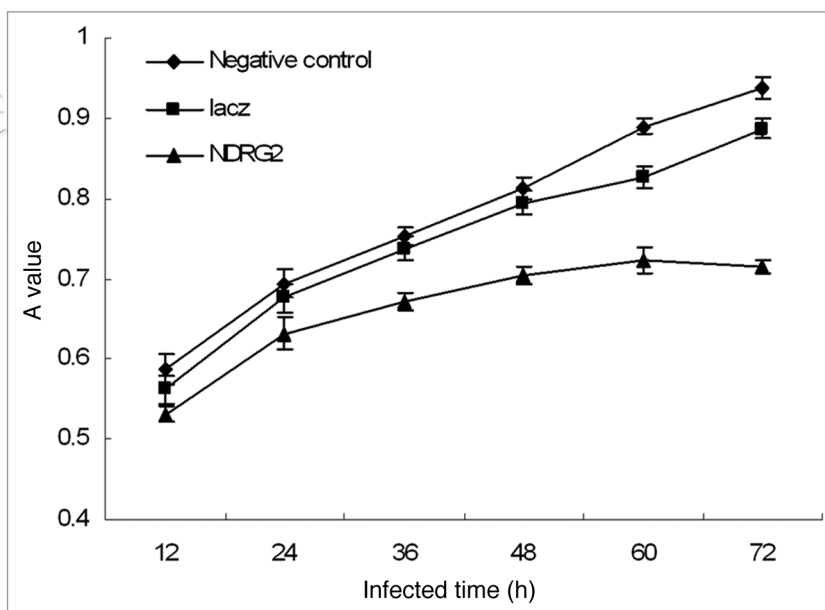


Figure 5. Cell growth curves. The cell growth curves are based on the average absorbance values ($n = 6$) detected with an autokinetic enzyme scaling meter and using the MTT method. All the assays were repeated in at least three independent experiments. The results are shown as the mean \pm SD.

The collection and use of human prostatic tissues were approved by the Fourth Military Medical University medical ethics committee. All patients provided written informed consent. Each tumor was scored for pathological stage based on the Gleason system, which was introduced in 1984 by Gleason. All of the samples had been reviewed and given a final diagnosis by three different clinical pathologists. The distribution of Gleason scores, pathologic-tumor-node-metastasis (pTNM) stages and

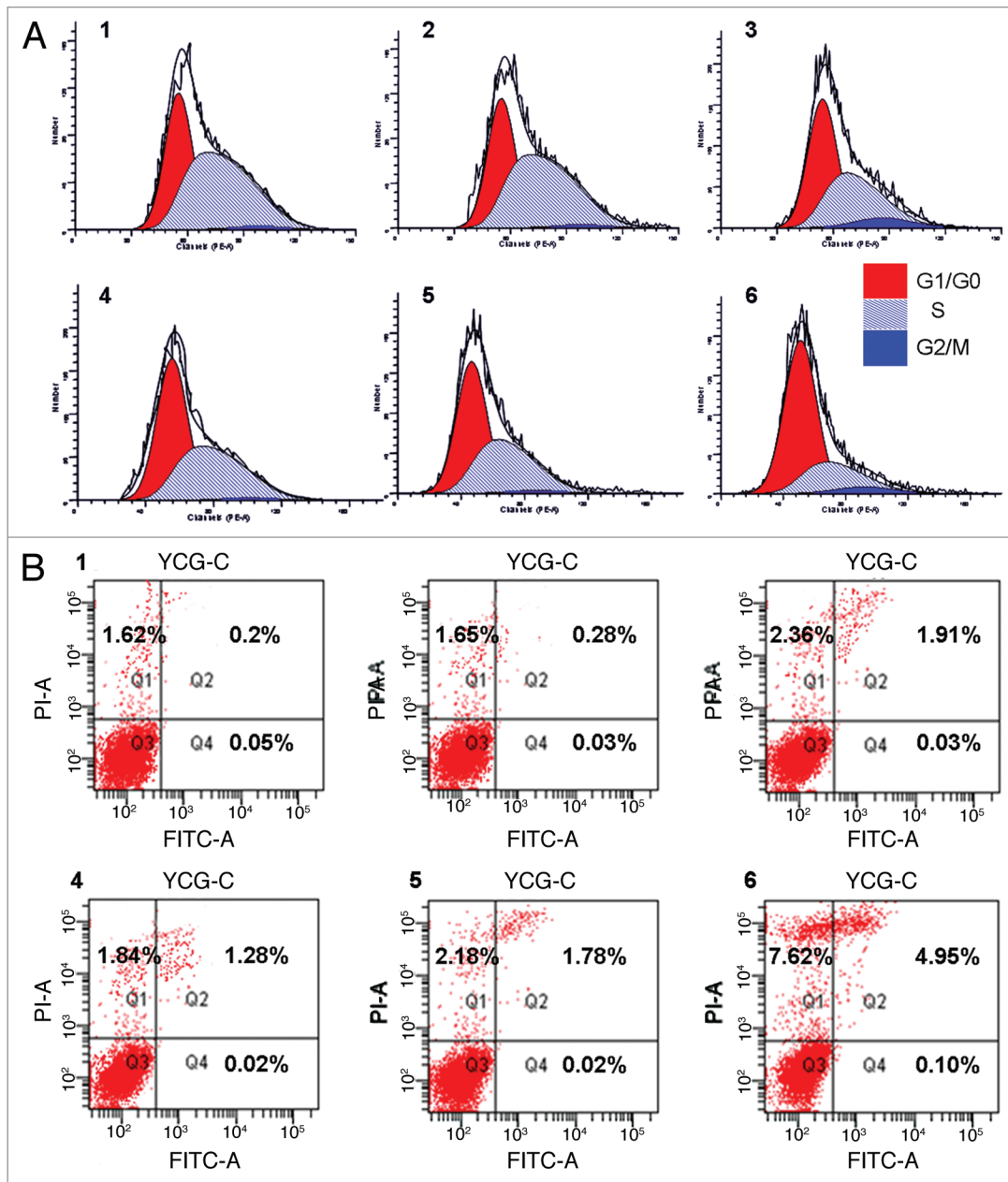


Figure 6. FCM assay of cell cycle arrest and apoptosis induced by NDRG2. (A) PC3 cells infected with pAd-cmv-NDRG2 adenovirus were more easily arrested in G₁/G₀ cycle. (B) Percentages of apoptotic cells in NDRG2 group were larger than in the other two groups. (1–3) 48 h after the infection; (4–6) 72 h after the infection; (1 and 4) blank control (PBS); (2 and 5) Lacz; (3 and 6) NDRG2. All the assays were repeated in least three independent experiments. The results are shown as the mean \pm SD.

serum concentrations of prostate-specific antigen (PSA) for the 107 PCAs are displayed in Table 2.

Immunohistochemistry. A mouse anti-human NDRG2 monoclonal antibody was purchased from Santa Cruz Biotechnology (CA). C-myc monoclonal antibody (mouse anti-human) and an immunohistochemistry kit were purchased from the Boster Company (Wuhan, CHN). The immunohistochemistry staining was performed according to the manufacturer's instructions. A BPH slide incubated with anti-actin primary antibodies served as the positive control, and a slide maintained in 0.01 mol/L PBS, instead of the primary antibody solution,

served as a negative control. A section of breast cancer tissue acted as a positive control for c-Myc staining.

Both the intensity and the extent of immunological staining were analyzed semi-quantitatively. Sections with no labeling or with fewer than 5% labeled cells were scored as 0. Sections were scored as a 1 if 5–25% of cells were labeled, as a 2 if 25–50% of cells were labeled, and as a 3 if 50–75% of cells were labeled. Finally, labeling of $\geq 75\%$ of the cells was scored as a 4. The staining intensity was scored similarly, with 0 used for negative staining, 1 for weakly positive, 2 for moderately positive and 3 for strongly positive. The scores for the percentage of positive

Table 3. Cell cycle arrest and cell apoptosis induced by pAD-cmv-NDRG2 on PC3 cells

Group	G ₀ /G ₁	G ₂ /M	S	Apoptosis
Blank control				
48 h	41.97 ± 1.19	2.11 ± 0.31	55.92 ± 1.77	1.77 ± 0.26
72 h	51.13 ± 2.14	2.28 ± 0.39	46.59 ± 2.89	3.01 ± 1.01
Lacz				
48 h	41.46 ± 1.50	2.05 ± 0.47	56.49 ± 1.95	1.89 ± 0.41
72 h	53.77 ± 3.49	2.35 ± 0.82	43.88 ± 3.83	3.95 ± 0.86
NDRG2				
48 h	51.29 ± 1.68*	6.99 ± 1.36*	41.72 ± 1.55*	3.97 ± 0.93*
72h	69.15 ± 3.27*	5.58 ± 1.23*	25.27 ± 3.02*	12.51 ± 2.53*

Data are presented as % (Mean ± SD, n = 4). Statistical significance was evaluated with ANOVA and SNK tests. *p < 0.001, compared with the controls.

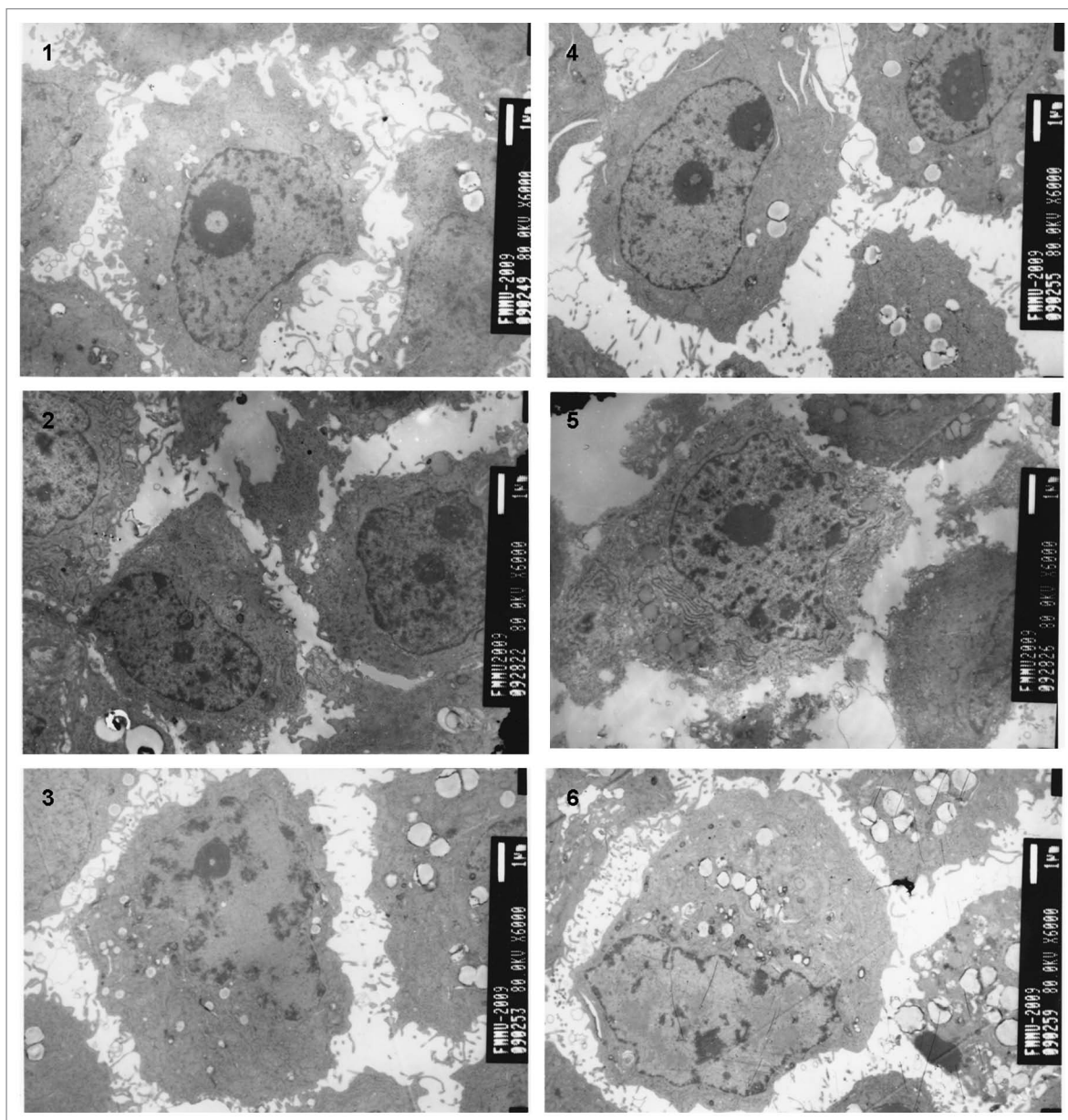


Figure 7. TEM-observed morphological changes of PC3 cells induced by NDRG2. The TEM micrographs showed that the nuclei became smaller and heterochromatin increased in the NDRG2 group and not the controls. (1–3) 48 h after the infection; (4–6) 72 h after the infection; (1 and 4) blank control (PBS); (2 and 5) Lacz; (3 and 6) NDRG2.

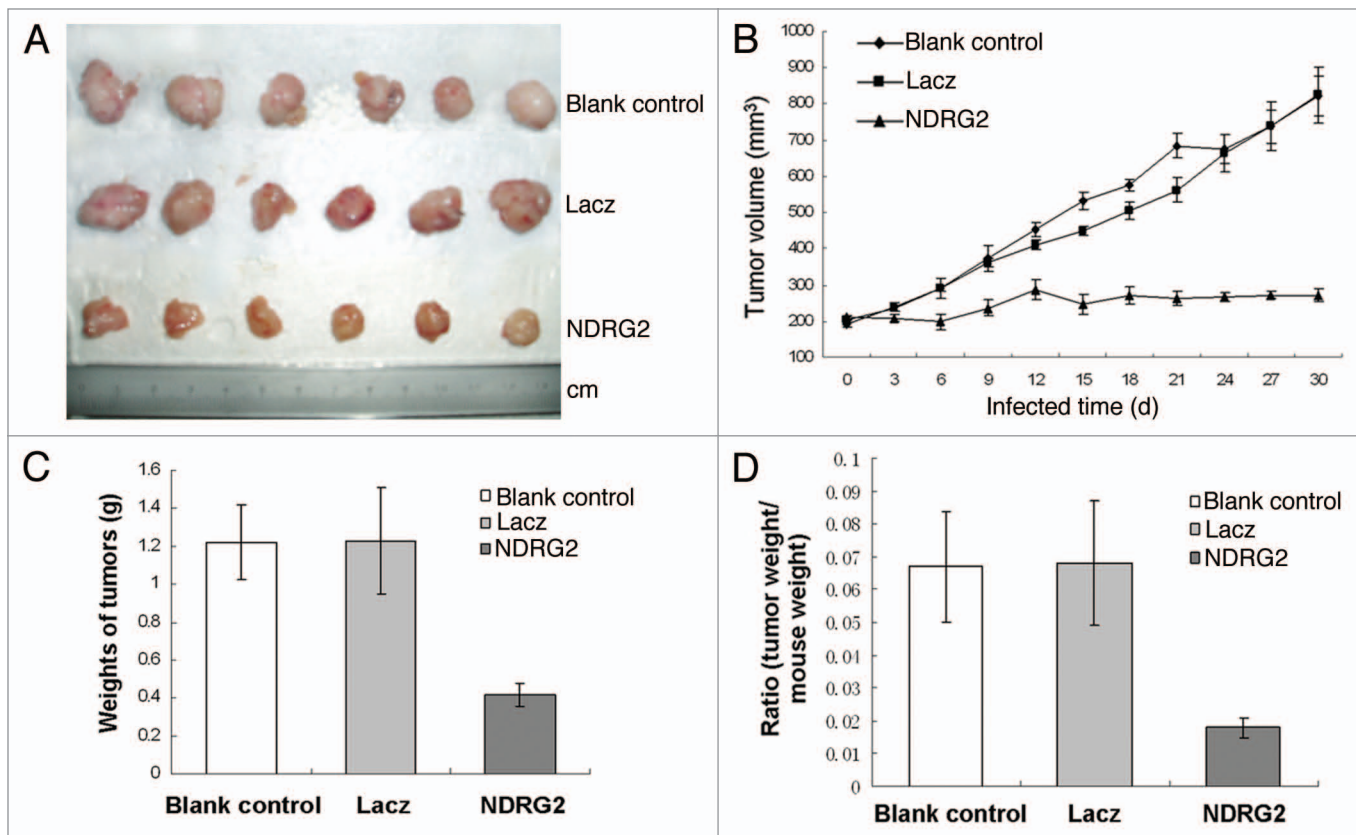


Figure 8. NDRG2 can suppress the growth of PC3 xenografts in vivo. (A) NDRG2 could suppress the growth of tumors compared to the two controls. (B) Tumor growth curves. (C) Masses of tumors in different groups. (D) Ratios of tumor masses to mouse masses in different groups. The curves and histograms were drawn based on the average values ($n = 6$) in different groups. The results are shown as the mean \pm SD.

cells and for the staining intensity were multiplied to generate an immunoreactive score for each specimen. The product of the quantity and intensity scores were calculated such that a final score of 0 indicated no expression, 1–4 indicated weak expression, 5–8 indicated moderate expression and 9–12 indicated strong expression. Each sample was examined separately and scored by two pathologists. Cases with discrepancies in the scores were discussed to reach a consensus. The photos were collected through light microscopy and SPOT Advanced Software (Olympus, Nagano, Japan).

Cell culture. PC3, LNCaP and DU145 are the most frequently used cell lines in the study of PCA, and we chose normal human prostate cells (RWPE2) as the control. After resuscitation, the cells were maintained in phenol red-free RPMI1640 (Gibco) containing 100 ml/L fetal bovine serum (Haoyang Tianjin, China) at 37°C in a humidified atmosphere with 50 ml/L CO₂ in air. When the cells grew to approximately 80% confluence in 25 cm² plastic culture flasks, we collected the cells through trypsinization.

Protein gel blot analysis. Protein gel blot was performed as follows. After extracting all of the protein of each of the cell lines with lysis buffer, the protein samples (40 μ g) were separated by SDS-PAGE at 12% concentration. Gels were electroblotted onto nitrocellulose membranes (Amersham, St. Giles, UK). After that, the blots were incubated with primary mouse anti-human

NDRG2 and c-Myc monoclonal antibody (1:500 dilution) for 1 h at room temperature and overnight at 4°C. GAPDH protein (36 kDa) detection was used as an internal control. The blots were then incubated with goat anti-mouse peroxidase-labeled antibodies (1:4,000 dilution; Santa Cruz Biotechnology, CA) for at least 1 h at room temperature. ECL detection solutions (Pierce, NJ) were then applied. Scanned images were quantified using Kodak Digital Science ID software (Kodak, NY).

Adenovirus infection. pAd-cmv-NDRG2, pAd-cmv-lacz and pAd-cmv-EGFP adenoviruses were packaged and purified in the biochemistry laboratory of our university (the titers were 1.3×10^{12} pfu/ml, 1.6×10^{12} pfu/ml and 1.0×10^{12} pfu/ml respectively). According to the results of protein gel blot, we successfully infected PC3 cells with the adenoviruses. pAd-cmv-EGFP adenovirus was used to determine the best multiplicity of infection (MOI) and the best time of infection. Moreover, we used pAd-cmv-NDRG2 to infect the PC3 cells and determine via protein gel blot whether the cells could express NDRG2 protein properly after infection. We also ascertained the differential expression of proteins that correlated with cell cycle stage and cell apoptosis at 48 and 72 h after infection (cell cycle protein: cyclinD1, CDK4; cell apoptosis protein: p21).

Cell growth inhibition tests in vitro. The tests included MTT assays, flow cytometry assays (FCM) (BD company, NJ) and transmission electron microscopy (TEM) (Hitachi, Tokyo, Japan).

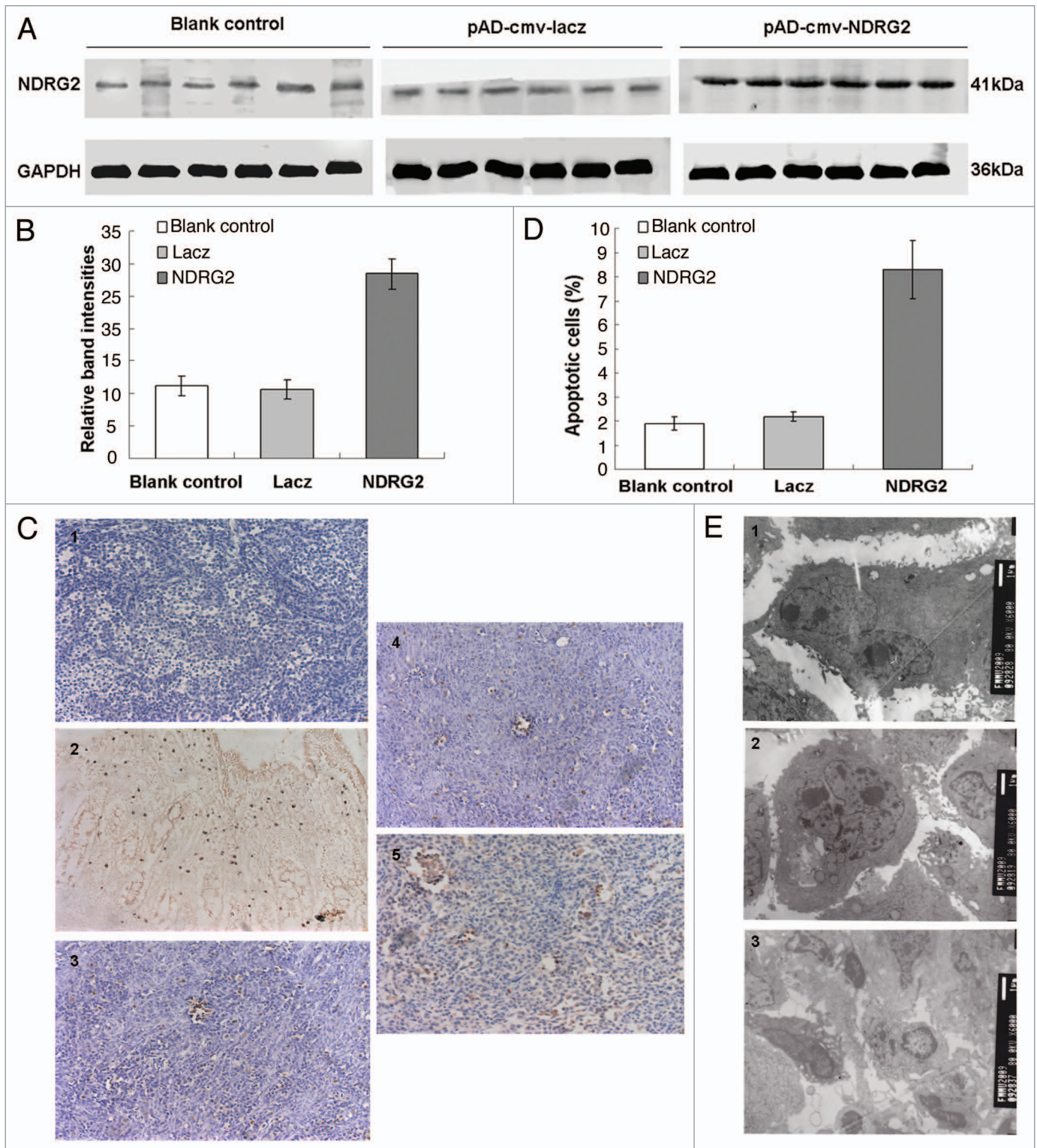


Figure 9. The effects of NDRG2 overexpression on PC3 xenografts as detected with further assays. (A) Differential expression of NDRG2 protein among groups assayed with protein gel blot. (B) Relative quantification of the expression NDRG2 protein in different groups, normalized to GAPDH levels. The assay was repeated in at least three independent experiments. The results are shown as the mean \pm SD. (C) Apoptotic cells detected with TUNEL staining (x200). (1) Negative control; (2) positive control (colon cancer tissue); (3) blank control (the tumors were treated with PBS substituting the adenovirus); (4) Lacz; (5) NDRG2. (D) Percentages of apoptotic cells in different groups. The histogram was drawn based on the average percentages of apoptotic cells in ten random visual fields in every group. The results are shown as the mean \pm SD. (E) Morphological changes of cells in PC3 xenografts induced by NDRG2 as observed with TEM. The TEM micrographs showed that the nuclei became smaller and heterochromatin increased in NDRG2 group compared to the controls. (1) Blank control (PBS); (2) Lacz; (3) NDRG2.

Each one was applied to each of the three groups (PBS-treated cells, the blank control; lacZ, the negative control; and NDRG2, the experimental group). (1) **MTT** assay: PC3 cells (3,000 cells/well) were inoculated in 96-well plates and every group had six reduplicative wells. The culture fluid was discarded 12, 24, 36, 48, 60 and 72 h after infection and 20 μ L/well (5 mg/mL) MTT solution was supplemented at 37°C for 4 h followed by 150 μ L/well DMSO, and shaken for 10 min. Absorbance (A) values were detected with an autokinetic enzyme scaling meter (Bio-Rad, CA) at 492 nm wavelength. Cell growth curves then were drawn based on the average A values. (2) **FCM**: PC3 cells (5×10^5 cells/well) were plated in 6-well culture dishes in the presence of different adenoviruses (at the suitable MOI). After 48 and 72 h, cells were harvested, centrifuged at low speed and fixed in 70% ethanol. After overnight incubation at 4°C, cells were stained with 50 μ g/ml propidium iodide in the presence of RNaseA (10 μ g/ml) and 0.1% Triton X-100, and measured with a flow cytometer. The experiments were repeated four times. (3) **TEM**: After treatment with adenovirus for 48 and 72 h, PC3 cells were digested by 0.25% trypsin and collected. Cells were rinsed with PBS and fixed with 3% glutaraldehyde for 30 min. After routine embedding and sectioning, cells were examined via electron microscopy.

Growth inhibition assays in vivo. Male BALB/c nude mice were purchased from Shanghai Experimental Animal Center, Chinese Academy of Sciences, Shanghai, China. PC3 cells were harvested and resuspended in sterile PBS. PC3 cells (1×10^7 in

0.2 mL were injected subcutaneously into the left flanks of the 6-week-old nude mice. When the mean size of tumors reached 200 mm³ (as calculated by the equation: $V[\text{mm}^3] = ab^2/2$) in the mice's bodies, all the mice were divided into three groups randomly (NDRG2, lacZ and control groups, n = 6 per group). Intratumoral injections of pAd-cmv-NDRG2 (1×10^9 pfu in 100 μ L PBS) adenovirus were made every 3 d for a total of nine times. After the injections, the mice were sacrificed by cervical dislocation and tumor specimens were taken, photographed, measured and weighed. The expression levels of NDRG2 protein in the inoculated tumors were detected using protein gel blot. The percentage of apoptotic cells was detected with TUNEL stain kit (Boster, Wuhan, China) according to the manufacturer's instructions. Immunolabeling was visualized by reaction via DAB, with the nuclei of apoptotic cells being stained brown. Ten visual fields were chosen randomly in every group and the numbers of positive cells were counted. Changes in the nuclei and organelles of the tumor cells were detected by TEM.

Statistical analysis. Statistical analyses were performed with SPSS13.0 software (SPSS company, IN). For immunohistochemistry results, disparities across groups were analyzed using Chi-square tests and Pearson correlation coefficient. Analysis of variance (ANOVA) and Student-Newman-Keuls (SNK) tests were computed to determine whether there were differences among the results of assays in vitro and in vivo. A p value less than 0.05 was considered statistically significant.

References

- Rubin MA. Targeted therapy of cancer: new roles for pathologists-prostate cancer. *Mod Pathol* 2008; 21:44-55.
- Shimono A, Okuda T, Kondoh H. N-myc-dependent repression of *ndr1*, a gene identified by direct subtraction of whole mouse embryo cDNAs between wild type and N-myc mutant. *Mech Dev* 1999; 83:39-52.
- Zhou RH, Kokame K, Tsukamoto Y, Yutani C, Kato H, Miyata T. Characterization of the human NDRG gene family: a newly identified member, NDRG4, is specifically expressed in brain and heart. *Genomics* 2001; 73:86-97.
- Deng Y, Yao L, Chau L, Ng SS, Peng Y, Liu X, et al. N-myc downstream-regulated gene 2 (NDRG2) inhibits glioblastoma cell proliferation. *Int J Cancer* 2003; 106:342-7.
- Deng YC, Wang JC, Liu XP, Ji SP, Yao LB. Cloning tumor-related genes and tumor suppressor genes in glioma with polymerase chain reaction-based subtractive hybridization. *Ai Zheng* 2005; 24:680-4.
- Piepoli A, Cotugno R, Merla G, Gentile A, Augello B, Quitadamo M, et al. Promoter methylation correlates with reduced NDRG2 expression in advanced colon tumor. *BMC Med Genomics* 2009; 2:11-5.
- Zhao H, Zhang J, Lu J, He X, Chen C, Li X, et al. Reduced expression of N-myc downstream-regulated gene 2 in human thyroid cancer. *BMC Cancer* 2008; 8:303-11.
- Teipel M, Roerig P, Wolter M, Gutmann DH, Perry A, Reifenberger G, et al. Frequent promoter hypermethylation and transcriptional downregulation of the NDRG2 gene at 14q11.2 in primary glioblastoma. *Int J Cancer* 2008; 123:2080-6.
- Ma J, Jin H, Wang H, Yuan J, Bao T, Jiang X, et al. Expression of NDRG2 in clear cell renal cell carcinoma. *Biol Pharm Bull* 2008; 31:1316-20.
- Park Y, Shon SK, Kim A, Kim KI, Yang Y, Cho DH, et al. SOCS1 induced by NDRG2 expression negatively regulates STAT3 activation in breast cancer cells. *Biochem Biophys Res Commun* 2007; 363:361-7.
- Foletta VC, Prior MJ, Stupka N, Carey K, Segal DH, Jones S, et al. NDRG2, a novel regulator of myoblast proliferation, is regulated by anabolic and catabolic factors. *J Physiol* 2009; 587:1619-34.
- Choi SC, Kim KD, Kim JT, Kim JW, Yoon DY, Choe YK, et al. Expression and regulation of NDRG2 (N-myc downstream regulated gene 2) during the differentiation of dendritic cells. *FEBS Lett* 2003; 553:413-8.
- Aggarwal R, Ryan CJ. Castration-resistant prostate cancer: targeted therapies and individualized treatment. *Oncologist* 2011; 16:264-75.
- Bracarda S, Logothetis C, Sternberg CN, Oudard S. Current and emerging treatment modalities for metastatic castration-resistant prostate cancer. *BJU Int* 2011; 107:13-20.
- Yao L, Zhang J, Liu X. NDRG2: a Myc-repressed gene involved in cancer and cell stress. *Acta Biochim Biophys Sin (Shanghai)* 2008; 40:625-35.
- Liu N, Wang L, Li X, Yang Q, Liu X, Zhang J, et al. N-Myc downstream-regulated gene 2 is involved in p53-mediated apoptosis. *Nucleic Acids Res* 2008; 36:5335-49.
- Zhang J, Li F, Liu X, Shen L, Liu J, Su J, et al. The repression of human differentiation-related gene NDRG2 expression by Myc via Miz-1-dependent interaction with the NDRG2 core promoter. *J Bio Chem* 2006; 281:39159-68.
- Yang G, Timme TL, Frolov A, Wheeler TM, Thompson TC. Combined c-Myc and caveolin-1 expression in human prostate carcinoma predicts prostate carcinoma progression. *Cancer* 2005; 103:1186-94.